Synlett D. R. Jones et al. Cluster

Novel Fluorescent Fluorene-Containing Conjugated Polymers: Synthesis, Photophysical Properties, and Application for the Detection of Common Bisphenols

Daniel R. Jones
Ryan Vallee
Mindy Levine*

Department of Chemistry, University of Rhode Island, 140 Flagg Road, Kingston, 02881, USA
m_levine@uri.edu

Published as part of the Cluster *Synthesis of Materials*

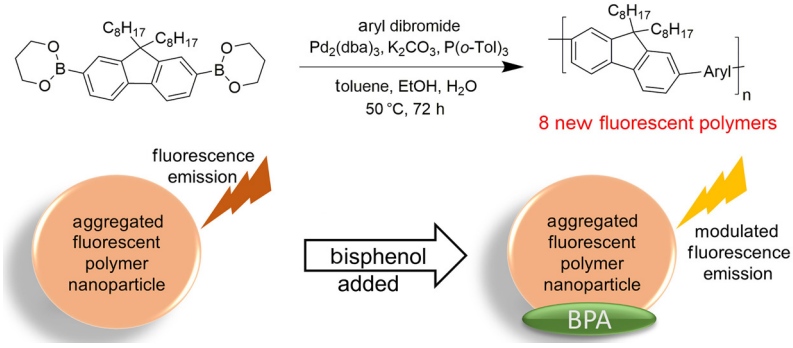

Received: 16.07.2018
Accepted after revision: 13.08.2018
Published online: 20.09.2018
DOI: 10.1055/s-0037-1609946; Art ID: st-2018-r0450-c

Abstract Eight new fluorescent conjugated polymers were synthesized by the Suzuki polycondensation reaction of 9,9-dioctylfluorene-2,7-diboronic acid bis(1,3-propanediol) ester and a conjugated dihalogenated monomer. The photophysical properties of these polymers were investigated as well-dissolved solutions in chloroform and as nanoparticle suspensions in water. Several of the polymers had large Stokes shifts (greater than 100 nm) and others demonstrated unique changes in the fluorescence properties in aggregated verse nonaggregated forms. Preliminary applications of these polymers in the detection of common bisphenols are also reported.

Key words polymers, nanostructures, aggregation, spectroscopy, conjugation

The synthesis of conjugated fluorescent polymers with extremely large (greater than 100 nm) Stokes shifts is of interest for a broad variety of applications, including gas sensing[1] and biological imaging.[2] Examples of fluorophores with large Stokes shifts have been reported in the literature,[3] and usually have charge-separated states[3b] or strong donor–acceptor coupling[3a] that are responsible for such large Stokes shifts. The practical advantage to large Stokes shifts is that such shifts generally lead to high signal-to-noise ratios as a result of the large separation between the emission signal and the excitation wavelength. Less research has focused on the synthesis and applications of conjugated polymers with analogously large Stokes shifts, with one reported example relying on the aggregation of a conjugated polymer to enable such shifts.[4] Nonetheless, conjugated polymers are well-known for their high sensitivity in fluorescence-based detection applications,[5] and so the ability to combine extremely large Stokes shifts with the notable advantages of conjugated polymer chemistry is expected to provide architectures with the combined advantages of high signal-to-noise ratios and increased fluorescence sensitivity.[6]

Previous work in our group has focused on the use of conjugated fluorescent polymers for the turn-on fluorescence detection of pesticides,[7] for the turn-off (i.e. quenching-based) fluorescence detection of nitroaromatics,[8] and for the highly sensitive detection of hydrogen peroxide via a noncovalent, electrostatically driven anionic polymer–cationic titanium detection complex.[9] All previously reported studies in the Levine group used polymers that were either commercially available or had been reported in the literature.[10] None of these polymers had notable Stokes shifts, and methods to achieve such large shifts by synthetic modification of the polymer architectures were relatively limited.

Many of the notable benefits of conjugated polymer-based sensors are enhanced when the polymer is in an aggregated state, such as nanoparticles. This enhancement is due to the increased availability of interpolymer exciton migration in addition to intra-polymer migration, resulting in markedly more sampling of the analyte binding sites by the generated excitons. Researchers have used the increased sensitivity of conjugated polymer nanoparticles (CPNs) for the detection of numerous analytes, including pesticides,[7] nitroaromatics,[8] and cations[11] at parts per billion (i.e. ppb) concentrations.[12] This interest is driven by the typically high fluorescence quantum yield of CPNs (~80%),[3] low toxicity to biological systems,[4] and ability to achieve aggregation-induced emission of conjugated fluorescent polymers when localized as nanoparticles.[5] Additionally, the modular design of conjugated fluorescent polymers and the ability to control the size of CPNs by straightforward experimental manipulation provides a system that is highly tunable and can be easily optimized.

One family of analytes of particular interest as detection targets is bisphenols. The most commonly used bisphenol is Bisphenol A (BPA, compound **1**), with over five million tons of compound **1** manufactured worldwide per year.[13] This prevalence has led to a chronic detectable level of BPA in biological fluids (i.e. urine, blood, saliva) from the majority of people living in developed nations.[13] Such ubiquitous BPA exposure is concerning, as BPA is a known estrogen mimic and endocrine disruptor.[14] Numerous studies have linked chronic low dose exposure to BPA to numerous negative health effects including prostate and breast cancer, obesity, early onset puberty, and Type II diabetes.[15] Regulatory changes and consumer-driven pressure over the health effects of BPA have caused companies to replace BPA with other bisphenols (BPs), such as bisphenol F (BPF, compound **2**) and bisphenol S (BPS, compound **3**).[16] The structural similarity and initial research on these BPs suggest that they have similar or more severe negative health effects compared to BPA, **1**.[16] Current methods for detecting BPs include gas chromatography coupled with mass spectrometry (GC–MS),[17] liquid chromatography coupled with mass spectrometry (LC–MS),[18] and electrochemical techniques.[19] GC–MS and LC–MS techniques are costly and time-consuming, while electrochemical techniques for the detection of bisphenols require large overpotentials that damage electrodes and reduce the system sensitivity and selectivity.[20] Newer BPA detection methods,[21] including chemiluminescent sensors,[22] have also been reported.

Reported herein is the synthesis and photophysical characterization of eight new fluorescent polymers and their application for the fluorescence detection of common BPs. The use of Suzuki coupling to synthesize conjugated fluorescent polymers is well-precedented in the literature to access a number of polymeric architectures,[23] and has significant advantages compared to other synthetic methods, including relative insensitivity to air and moisture, high functional group tolerance, and generally high yields.[24] Of the eight new architectures, four demonstrated Stokes shifts greater than 100 nm, and three of the new polymers had significantly different fluorescence responses based on their level of aggregation. All polymers displayed some degree of fluorescence changes with the addition of BPA, BPF, or BPS (compounds **1**–**3**, Figure 1), as both aggregated polymer nanoparticles and well-dissolved polymer solutions. Notably, 100% differentiation between the bisphenols was observed using linear discriminant analysis of the resulting fluorescence response signals.

The solubility of conjugated polymers can pose problems in post-synthesis processing, as the propensity of the conjugated chains to π-stack and aggregate leads to low solubility in most solvents. Options to enhance polymer solubility include the incorporation of sterically bulky side chains,[25] which reduces aggregation, and the inclusion of highly polar functional groups,[26] which increases the polymer solubility in polar solvents. Undesired effects of incorporating sterically bulky or polar substituents include added synthetic challenges[27] to access more functionalized monomers, as well as difficulties in forming conjugated polymer nanoparticles by hydrophobic collapse of the polymer chain, as a result of the lower hydrophobicity of the highly polar groups.[28]

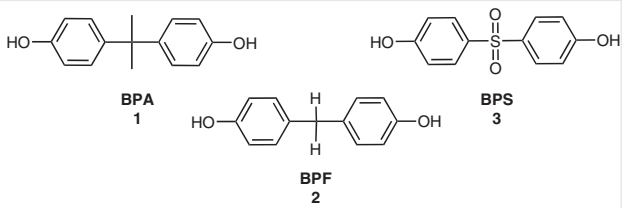

Figure 1 Structures of bisphenol analytes

Our fluorene containing polymers include only the two solubilizing hydrocarbon side chains found on 9,9-dioctylfluorene-2,7-diboronic acid bis(pinacol) ester (compound **4**, Scheme 1) and no solubilizing polar groups. A range of optimized conditions from literature-reported studies[29] were employed in an attempt to increase polymer weight (M_n) without increasing the number of solubilizing side chains. Scheme 1 illustrates the general reaction used for the optimization experiments, with the results of these experiments summarized in Table 1. The use of palladium zero complexes and tri(*o*-tolyl) phosphine ligands successfully increased the weights (M_n) of the polymers, with the combination of the two resulting in the second highest polymer weight (M_n = 5000 g/mol). For **P1**, this molecular weight corresponds to approximately 10 monomer units, and is comparable to the molecular weights of some other conjugated polymers reported in the literature.[10] Moreover, literature precedent indicates that the photophysical properties of longer-chain conjugated polymers are comparable to those of shorter-chain oligomers, with an oligomer of five repeat units often displaying photophysical properties that are indistinguishable from that of the full-length polymer.[30] Finally, by removing ethanol and using the phase-transfer catalyst tetra-*n*-butylammonium bromide (TBAB) with tris(dibenzylideneacetone)dipalladium(0) and tri(*o*-tolyl) phosphine as the ligand the highest polymer weight was achieved (experiment number 11, Table 1).[31]

The photophysical and structural properties of all synthesized polymers (Figure 2) were characterized as well-dissolved solutions and as aggregated nanoparticles. Of note, all polymers demonstrated measurable fluorescence emission from excitation at or near the maximum absorption wavelength, with key results summarized in Table 2.

Polymer **P1** has a large Stokes shift of over 200 nm and is characterized by a relatively low molecular weight, likely due to limitations on the solubility of the monomers and polymer. Polymer **P2** was designed to increase the polymeric molecular weight while maintaining a large Stokes shift,

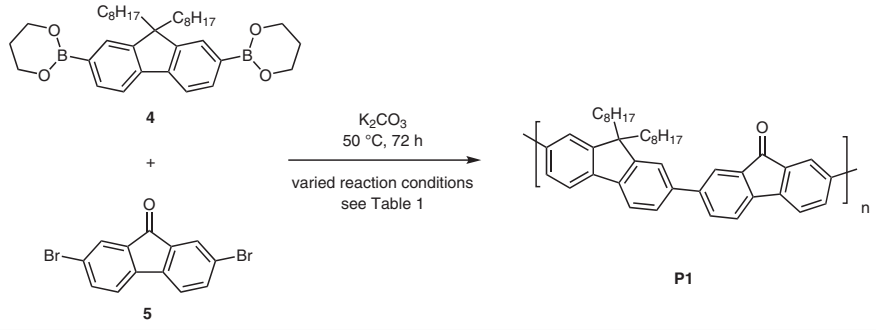

Scheme 1 Synthesis of **P1**

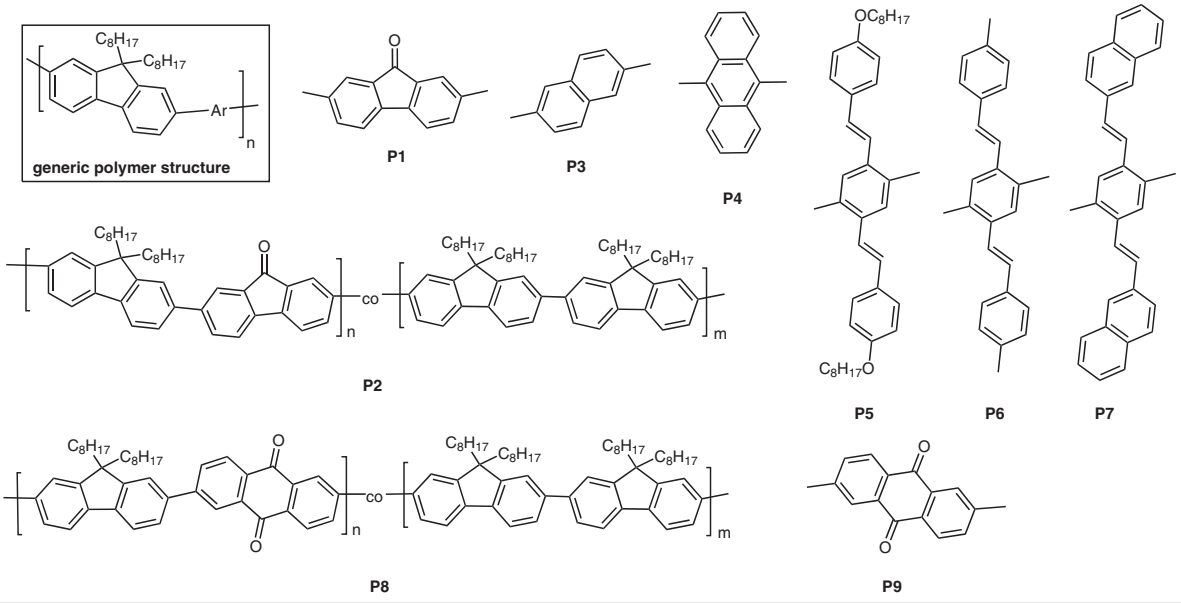

Figure 2 Structures of newly synthesized polymers

similar to that of **P1**. This goal was achieved successfully by increasing the number of alkyl-branched monomer units to a 3:1 ratio of dioctylfluorene/fluorenone (Figure 2, **P2**) in a random copolymer structure. This increased the polymer weight (M_n) by a factor of approximately five (taking into account the larger molecular weight of the monomer repeat units) while still retaining the large Stokes shift observed in **P1** (Stokes shifts: **P1** = 236 nm, **P2** = 230 nm). Interestingly, the random copolymer displayed an additional fluorescence emission peak with a smaller Stokes shift of 34 nm. This peak (at 414 nm) matches the fluorescence emission of poly-9,9-dioctylfluorene[32] and the second peak (at 610 nm) matches the fluorescence emission of 9-fluorenone.[33] When **P2** is aggregated as nanoparticles, the emission peak at 414 nm disappears and the peak at 610 nm undergoes a hypsochromic shift to 550 nm, (Figure 3), indicating energy transfer from 9,9-dioctylfluorene monomer units (with emission at 414 nm) to 9-fluorenone (with lower energy emission). This energy transfer is facilitated in the aggregated state because of facile interchain exciton migration that is enabled in such architectures.

Polymer **P3**'s UV absorbance and fluorescence emission were visually similar to the spectra of polymers with significant amounts of dioctylfluorene units (**P2** and **P8**). However, **P3** has a much higher quantum yield (0.7650) than **P2** (0.0058) and **P8** (0.0025), which is qualitatively similar to the quantum yields of all fluorene conjugated polymers, and has the smallest Stokes shift (33 nm) of all the investigated polymers. The UV absorbance and fluorescence emission characteristics of **P3** are of particular interest when compared to polymer **P4**, as both **P3** and **P4** include fused aromatic backbone segments in addition to their dioctylfluorene segments. However, their fused aromatic backbone segments result in vastly different photophysical properties. Polymer **P4** incorporates an unsubstituted anthracene moiety into its polymer backbone, resulting in **P4**'s UV absorbance being similar to anthracene's,[34] which indicates

Table 1 Summary of Reaction Optimization Experiments Using **P1** as the Polymer Target

Exp.	Conditions[a]			Results[b]		
	Catalyst and ligand	Monomer conc. (mol/L)	Solvents	M_n (g/mol)	M_w (g/mol)	PDI
1[c]	$Pd(OAc)_2$ (0.15 mol equiv) PPh_3 (0.45 mol equiv)	0.033	1:1:1 ethanol/toluene/water	2700	3800	1.41
2	$Pd(OAc)_2$ (0.15 mol equiv) PPh_3 (0.45 mol equiv)	0.033	1:1:1 ethanol/toluene/water	2600	4200	1.58
3	$Pd(OAc)_2$ (0.15 mol equiv) PPh_3 (0.45 mol equiv)	0.022	1:1 chloroform/water	2300	3500	1.52
4	$Pd(OAc)_2$ (0.15 mol equiv) PPh_3 (0.45 mol equiv)	0.033	1:2 chloroform/water	1800	2100	1.20
5	$Pd(PPh_3)_4$ (0.15 mol equiv)	0.033	1:1:1 ethanol/toluene/water	4700	5600	1.19
6	$Pd(OAc)_2$ (0.15 mol equiv) P(*o*-Tol)$_3$ (0.30 mol equiv)	0.033	1:1:1 ethanol/toluene/water	3200	5400	1.66
7	$Pd_2(dba)_3$ (0.15 mol equiv) PPh_3 (0.45 mol equiv)	0.033	1:1:1 ethanol/toluene/water	2800	3900	1.38
8	$Pd_2(dba)_3$ (0.15 mol equiv) P(*o*-Tol)$_3$ (0.30 mol equiv)	0.033	1:1:1 ethanol/toluene/water	5000	6500	1.30
9	$Pd(PPh_3)_4$ (0.15 mol equiv)	0.010	1:1:1 ethanol/toluene/water	3200	4200	1.29
10	$Pd(PPh_3)_4$ (0.15 mol equiv)	0.005	1:1:1 ethanol/toluene/water	3100	4400	1.43
11	$Pd_2(dba)_3$ (0.15 mol equiv) P(*o*-Tol)$_3$ (0.30 mol equiv) TBAB (1 mol equiv)	0.033	1:1 toluene/water	5800	8200	1.40

[a] All reactions were heated at 50 °C for 72 h and used K_2CO_3 (3 mol equiv) as the base.
[b] All results were obtained on an Agilent 1260 Infinity II Multi-Detector GPC/SEC System with a polystyrene internal standard.
[c] Experiment 1 was heated at 111 °C for 72 h.

that the anthracene segment of **P4** is absorbing more than the dioctylfluorene segment. This is in contrast to **P3**, which contains an unsubstituted naphthalene backbone segment, but does not absorb at wavelengths typical of naphthalene (311 nm).[35] Furthermore, **P4**'s fluorescence emission maximum is close to **P3**'s, resulting in a very large Stokes shift (178 nm) for **P4**. These small structural changes which result in large differences in the photophysical properties of the polymers demonstrate excellent tunability for tailoring the polymer products for specific applications.

Table 2 Properties of Fluorescent Polymers **P1**–**P9** Synthesized Using the Optimized Reaction Conditions[a]

Polymer	M_n (g/mol)	M_w (g/mol)	PDI	UV λ_{max} (nm)	Stokes shift (nm)		Fluorescence emission (nm)		Quantum yield[b]
					Fl λ_{max} 1	Fl λ_{max} 2	λ_{max} 1	λ_{max} 2	
P1	5000	6500	1.30	374	236	–	610	–	0.0056
P2	26400	49300	1.87	380	34	230	414	610	0.0068
P3	5300	14300	2.69	378	33	–	411	–	0.7650
P4	3000	4200	1.45	262	178	–	440	–	0.1403
P5	4800	8000	1.64	345	79	102	424	447	0.8278
P6	6000	12400	2.07	341	72	95	413	436	0.5918
P7	3200	5700	1.79	374	53	75	427	449	0.9080
P8	21500	59200	2.74	377	38	287	415	664	0.0025
P9	6700	9800	1.46	353	223	–	576	–	0.3087

[a] All reactions were heated at 50 °C for 72 h and used K_2CO_3 (3 mol equiv), $Pd_2(dba)_3$ (0.15 mol equiv), P(*o*-Tol)$_3$ (0.30 mol equiv), and two monomers (1 mol equiv each) at 0.033 mol/L in equal amounts ethanol, toluene, and water.
[b] Quantum yields were measured by using an integration sphere with the following references: 9,10-diphenylanthracene, quinine bisulfate, and 2-aminopyridine.

Polymers **P5** and **P6** have similar photophysical properties, with UV absorbance maxima at 345 and 341 nm, respectively. Both polymers have two fluorescence emission maxima (**P5** = 424, 447 nm; **P6** = 414, 436 nm) and large Stokes shifts (**P5** = 79, 102 nm; **P6** = 72, 95 nm). The differences in wavelength between the photophysical properties of **P5** and **P6** are expectedly small as the structural difference between the two polymers is an alkoxy versus an alkane functional group neither of which is on the polymer backbone.

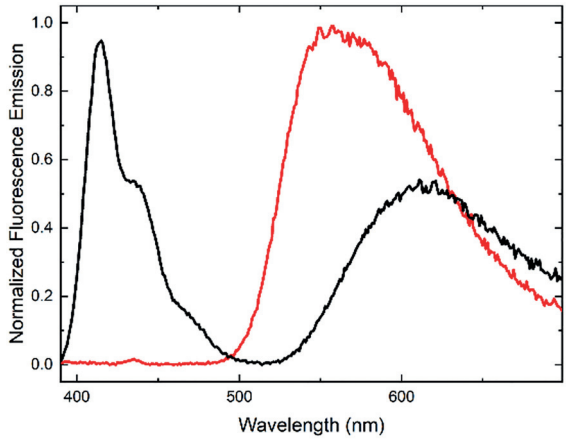

Figure 3 Normalized fluorescence emission of **P2** as a well-dissolved solution in chloroform (0.01 mg/mL) (black line) and as a nanoparticle suspension in water (red line) (λ_{ex} = 380 nm)

Interestingly, **P7**'s fluorescence emission changed from a spectrum with two emission maxima when dissolved in chloroform to a spectrum with much greater fine structure upon aggregation in nanoparticles, with four distinct maxima observed (Figure 4). The emission spectrum with four maxima shows the same fine structure as the fluorescence emission of naphthalene[36] and has a bathochromic shift of 42 nm compared to the nonaggregated state, which suggests J-aggregate formation.[37] These spectral features strongly suggest a geometric arrangement in which the polymer chains stack in a staggered arrangement with the pendant naphthalene moieties of **P7** directly above and below the fluorene backbone segments from neighboring polymer chains.

Polymers **P8** and **P9** are comprised of the same monomer units, albeit with different ratios of monomer in the polymer product (**P9**: 1:1 monomer ratio; **P8**: 3:1 ratio of 9,9-dioctylfluorene to anthraquinone monomer, Figure 2). Interestingly, **P8** displays two emission maxima at 414 nm and at 664 nm, while **P9** has only one emission peak at 576 nm. In a well-solubilized polymer solution, the fluorescence emission peak of **P8** at 664 nm accounts for less than 10% of the total fluorescence emission. However, similar to **P2**, the aggregated form of **P8** only displays one emission peak, at

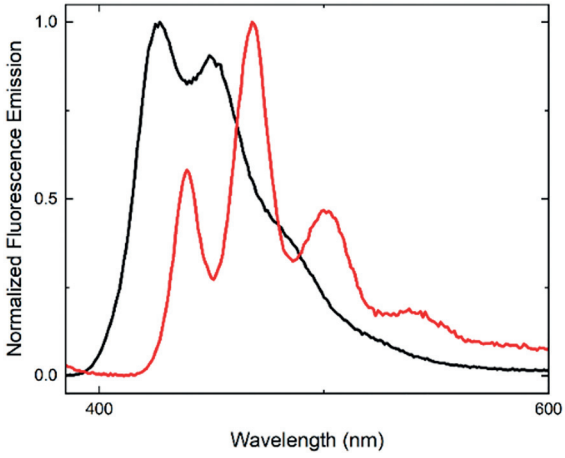

Figure 4 Normalized fluorescence emission of **P7** as a well-dissolved solution in chloroform (0.01 mg/mL) (black line) and a nanoparticle suspension in water (red line), (λ_{ex} = 375 nm)

570 nm, which is a significant hypsochromatic shift (94 nm) compared to the nonaggregated form. The large Stokes shift of **P9** (223 nm) contrasts with the double Stokes shifts for polymer **P8** (due to the dual emission) of 38 and 287 nm. Additionally, **P8**'s larger ratio of 9,9-dioctylfluorene monomer **4** compared to **P9**'s 1:1 monomer ratio results in **P8** having a polymer weight approximately 2.5 greater than that of **P9**, while still displaying fluorescence properties that are comparable to **P9** in the aggregated state.

In addition to characterizing the polymer's photophysical properties, all polymers were screened for their ability to detect BPA, BPF, and BPS (compounds **1**–**3**).[38] The fluorescence modulation[39] of the polymers in the presence of these analytes was measured as both well-dissolved chloroform solutions and as nanoparticles suspended in water. All polymers demonstrated some degree of fluorescence modulation in the presence of at least two bisphenols (Tables 3 and 4). The fluorescence response of **P1**, a previously reported polymer, to all bisphenol analytes is included in the Supporting Information for this manuscript.

All polymers demonstrated some degree of fluorescence modulation when they were dissolved in chloroform; however, high analyte concentrations (1 mM) were required to achieve measurable fluorescence responses. Moreover, poor selectivity between structurally similar analytes was observed, with half of the polymers, when dissolved in chloroform, displaying nearly identical modulation values with all analytes investigated. Polmer **P2** had one of the largest fluorescence modulations as a chloroform solution with the addition of BPS, with a modulation value of 1.48 obtained (Figure 5, a), whereas **P6** was one of the most selective as a chloroform solution, with noticeably different fluorescence spectra obtained for all bisphenol analytes (Figure 5, b). Additionally, **P4** showed similar selectivity to that of **P6** and a similarly large fluorescence modulation to that of **P2**, with

modulation values for **P4** chloroform solution varying between 0.39 and 0.49. These fluorescence responses are promising as the intermolecular forces that drive the bisphenols to interact with the polymers are less prevalent in chloroform solution than in aggregated states. Impressively, linear discriminant analyses of the relatively minor changes in spectral signals of the analyte–polymer complexes resulted in 100% successful differentiation of highly structurally similar analytes (Figure 6).

Table 3 Fluorescence Modulation of Polymers Dissolved in Chloroform with 1000 μM Bisphenol[a]

Polymer	BPA	BPF	BPS
P2	0.99	0.98	1.48
P3	0.98	1.02	1.06
P4	0.44	0.49	0.39
P5	0.82	0.80	0.80
P6	0.83	0.78	0.76
P7	0.98	0.98	0.98
P8	0.98	0.97	0.97
P9	0.98	0.96	0.98

[a] 0.5 mL of 1000 μM bisphenol in chloroform added to 2.0 mL 0.01 mg/ml polymer solution in chloroform. All modulation values were calculated according to fluorescence modulation = $Fl_{analyte}/Fl_{blank}$.[37]

Table 4 Fluorescence Modulation of Polymer Nanoparticles Suspended in Water with 50 μM Bisphenol[a]

Polymer	BPA	BPF	BPS
P2	1.03	1.05	1.04
P3	2.90	2.94	0.74
P4	0.92	1.06	1.00
P5	0.87	1.03	0.84
P6	0.46	0.54	1.00
P7	0.98	1.07	0.96
P8	0.81	0.79	0.80
P9	0.96	0.97	0.97

[a] 0.5 mL of 50 μM bisphenol in water added to 2.0 mL nanoparticle solution in water. All modulation values were calculated according to fluorescence modulation = $Fl_{analyte}/Fl_{blank}$.[37]

While the chloroform solutions demonstrated sufficient fluorescence modulation to differentiate between the bisphenols at high concentrations, the polymer nanoparticles had markedly enhanced selectivity to the bisphenol analytes at far lower analyte concentrations. This greater selectivity is driven by hydrophobic aggregation of the bisphenols with the polymer nanoparticles and the higher propensity for interpolymer exciton migration in aggregated

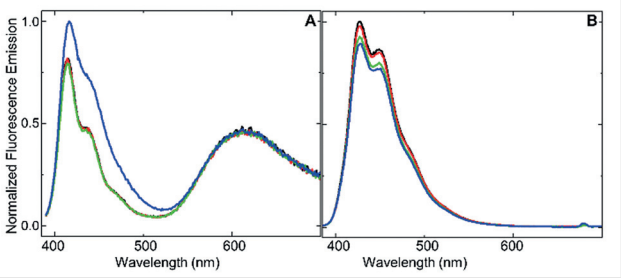

Figure 5 Normalized fluorescence emission of (A) **P2** and (B) **P6** as well-dissolved chloroform solutions (0.01 mg/mL) with: no analyte (black line), 1000 μM BPA (red line), 1000 μM BPF (green line), and 1000 μM BPS (blue line), (**P2** λ_{ex} = 380 nm, **P6** λ_{ex} = 340 nm)

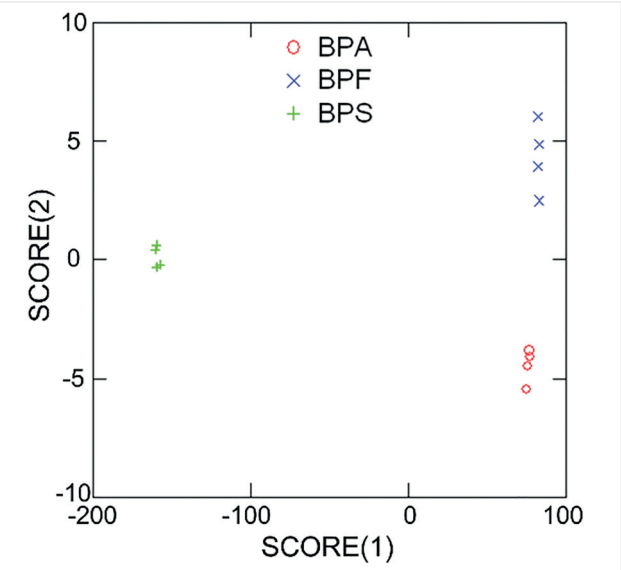

Figure 6 Statistical array of polymers in chloroform solution with 1000 μM bisphenols

states, which increases the number of analyte binding sites that the exciton samples prior to relaxation to the ground state.[40] The enhanced fluorescence modulation is seen with nearly all polymer nanoparticles–analyte combinations, except **P4** and **P6** with BPS, and current efforts in our laboratory are focused on elucidating reasons for the aberrant behavior of these particular combinations. Particularly notable fluorescence modulation is seen with polymer **P3** and **P5** nanoparticles (Figure 7). Polymer **P3** demonstrates the most pronounced fluorescence modulation of all nanoparticles, whereas **P5** has the greatest selectivity of all nanoparticle solutions between the less bulky BPF and the bulkier BPS and BPA. The difference in the selectivity of these polymers suggests that the electron-rich **P3** is interacting with the BPs primarily through electronic complementarity, whereas the fluorescence responses of **P5** are likely due to sterically driven interference between **P5**'s side chains and the BP analytes that disrupts the polymer aggregation.[41] Furthermore, when the fluorescence emis-

sion of the nanoparticles in the presence of the analytes was analyzed by using linear discriminant analysis (Figure 8), 100% differentiation between the three bisphenols at low concentrations (50 µM) was obtained. Finally, the stability of the nanoparticles in water was observed over 72 hours by DLS and no significant degradation or precipitation of the nanoparticles was observed. This is consistent with literature reported longevity studies of conjugated polymer nanoparticles generally remaining stable for weeks in aqueous solution.[42]

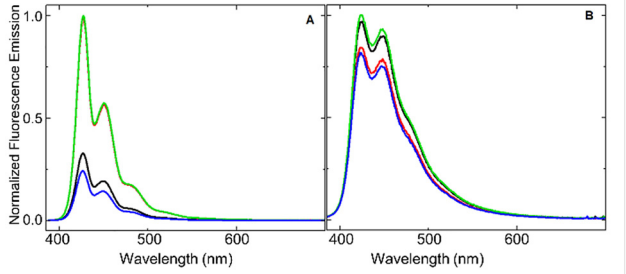

Figure 7 Normalized fluorescence emission of (A) **P3** and (B) **P5** as nanoparticles suspended in water with: no analyte (black line), 50 µM BPA (red line), 50 µM BPF (green line), and 50 µM BPS (blue line) (**P3** λ_{ex} = 378 nm, **P5** λ_{ex} = 345 nm)

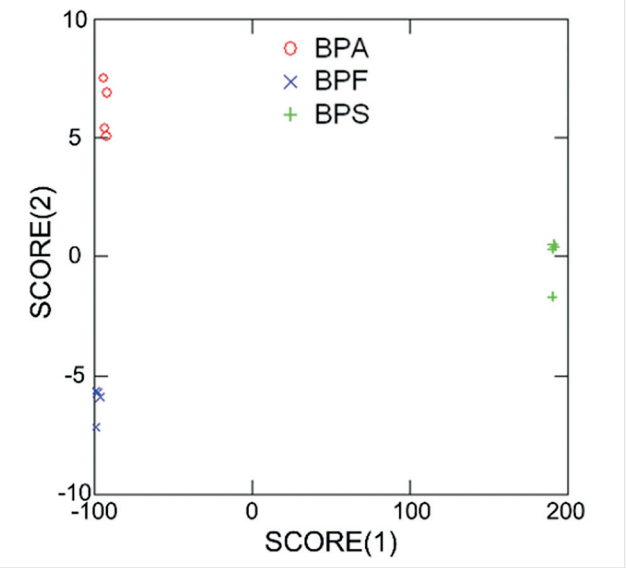

Figure 8 Statistical array of polymer nanoparticles in water with 50 µM bisphenols

In summary, eight new fluorescent polymers were synthesized by using Suzuki polycondensation. All eight polymers were spectroscopically characterized and their potential use as fluorescent sensors was investigated. Polymers **P2**, **P4**, **P5**, and **P9** had Stokes shifts that were greater than 100 nm, with a range of UV-vis absorbance maxima. Polymers **P2**, **P7**, and **P8** demonstrated significantly different fluorescence emission in aggregated states (i.e. in nanoparticles) compared to their fluorescence emission profiles as well-dissolved solutions in chloroform. The fluorescence responses of the polymers to the addition of BPA, BPF, and BPS were investigated, both for well-dissolved polymer solutions and as aggregated polymer nanoparticles. The polymers demonstrated some degree of fluorescence modulation in the vast majority of polymer–analyte parings with isolated analyte–polymer pairs demonstrating little to no observed modulation. With use of linear discriminant analysis, these distinctive fluorescence responses could differentiate between the three bisphenols with 100% selectivity, even among highly structurally similar analytes. Efforts towards extending this fluorescence-based detection system to other common environmental toxicants as well as evaluating the use of polymeric thin films for such sensing applications are currently underway in our laboratory. Further efforts towards determining the selectivity and robustness of this system by evaluating the system in complex aqueous media and expanding the analyte scope to other aromatic compounds both with and without bisphenols as competitive analyte studies will be performed, and the results of these and other investigations will be reported in due course.

Funding Information

The authors acknowledge the University of Rhode Island chemistry department for funding of this work.

Acknowledgment

The authors thank Dr. Matthew Kiesewetter and Mr. Kurt Fastnacht at the University of Rhode Island for the use of Dr. Kiesewetter's Agilent 1260 Infinity II Multi-Detector GPC/SEC System. We would like to thank Dr. William Euler for the use of his Malvern Zetasizer Nano ZS.

Supporting Information

Supporting information for this article is available online at https://doi.org/10.1055/s-0037-1609946.

References and Notes

(1) (a) Liu, S.-Y.; Qi, X.-L.; Lin, R.-B.; Cheng, X.-N.; Liao, P.-Q.; Zhang, J.-P.; Chen, X.-M. *Adv. Funct. Mater.* **2014**, *24*, 5866. (b) Divya Madhuri, U.; Radhakrishnan, T. P. *Dalton Trans.* **2017**, *46*, 16236.
(2) (a) Xiong, L.; Cao, F.; Cao, X.; Guo, Y.; Zhang, Y.; Cai, X. *Bioconjugate Chem.* **2015**, *26*, 817. (b) Choi, H. S.; Kim, Y.; Park, J. C.; Oh, M. H.; Jeon, D. Y.; Nam, Y. S. *RSC Adv.* **2015**, *5*, 43449.
(3) (a) Wu, X.; Li, H.; Xu, Y.; Tong, H.; Wang, L. *Polym. Chem.* **2015**, *6*, 2305. (b) Ran, Q.; Ma, J.; Wang, T.; Fan, S.; Yang, Y.; Qi, S.; Cheng, Y.; Song, F. *New J. Chem.* **2016**, *40*, 6281. (c) Casey, A.; Ashraf, R. S.; Fei, Z.; Heeney, M. *Macromolecules* **2014**, *47*, 2279.
(4) Pal, K.; Sharma, V.; Sahoo, D.; Kapuria, N.; Koner, A. L. *Chem. Commun.* **2018**, *54*, 523.

(5) (a) Rochat, S.; Swager, T. M. *ACS Appl. Mater. Interfaces* **2013**, *5*, 4488. (b) Swager, T. M. *Macromolecules* **2017**, *50*, 4867.
(6) (a) Resch-Genger, U.; Rurack, K. *Pure Appl. Chem.* **2013**, *85*, 2005. (b) Wu, I.-C.; Yu, J.; Ye, F.; Rong, Y.; Gallina, M. E.; Fujimoto, B. S.; Zhang, Y.; Chan, Y.-H.; Sun, W.; Zhou, X.-H.; Wu, C.; Chiu, D. T. *J. Am. Chem. Soc.* **2014**, *137*, 173.
(7) Talbert, W.; Jones, D.; Morimoto, J.; Levine, M. *New J. Chem.* **2016**, *40*, 7273.
(8) Marks, P.; Cohen, S.; Levine, M. *J. Polym. Sci. A: Polym. Chem.* **2013**, *51*, 4150.
(9) Marks, P.; Radaram, B.; Levine, M.; Levitsky, I. A. *Chem. Commun.* **2015**, *51*, 7061.
(10) Bouffard, J.; Swager, T. M. *Macromolecules* **2008**, *41*, 5559.
(11) Feng, L.; Sha, J.; He, Y.; Chen, S.; Liu, B.; Zhang, H.; Lu, C. *Microporous Mesoporous Mater.* **2015**, *208*, 113.
(12) Li, S.; Chen, F.; Liu, F.; Liu, F.; Liu, Z.; Zeng, R.; Tang, H.; Gao, Z.; Zhou, H. *J. Liq. Chromatogr. Relat. Technol.* **2015**, *38*, 1474.
(13) Im, J.; Löffler, F. E. *Environ. Sci. Technol.* **2016**, *50*, 8403.
(14) Kundakovic, M.; Champagne, F. A. *Brain. Behav. Immun.* **2011**, *25*, 1084.
(15) Muhamad, M. S.; Salim, M. R.; Lau, W. J.; Yusop, Z. *Environ. Sci. Pollut. Res.* **2016**, *23*, 11549.
(16) Delfosse, V.; Grimaldi, M.; Pons, J.-L.; Boulahtouf, A.; Le Maire, A.; Cavailles, V.; Labesse, G.; Bourguet, W.; Balaguer, P. *Proc. Natl. Acad. Sci. U.S.A.* **2012**, *109*, 14930.
(17) Caballero-Casero, N.; Lunar, L.; Rubio, S. *Anal. Chim. Acta* **2016**, *908*, 22.
(18) (a) Zhao C., Xie P., Wang H., Cai Z.; *J. Hazard. Mater.*; **2018**, in press; DOI: 10.1016/j.jhazmat.2018.05.010. (b) Sun, F.; Kang, L.; Xiang, X.; Li, H.; Luo, X.; Luo, R.; Lu, C.; Peng, X. *Bioanal Chem.* **2016**, *408*, 6913.
(19) (a) Ling, L. J.; Xu, J. P.; Deng, Y. H.; Peng, Q.; Chen, J. H.; Ya, S. H.; Nie, Y. J. *Anal. Methods* **2018**, *10*, 2722. (b) Tan, F.; Cong, L.; Li, X.; Zhao, Q.; Zhao, H.; Quan, X.; Chen, J. *Sensors Actuators B: Chem.* **2016**, *233*, 599.
(20) Gao, Y.; Cao, Y.; Yang, D.; Luo, X.; Tang, Y.; Li, H. *J. Hazard. Mater.* **2012**, 199–200, 111.
(21) Hou, C.; Zhao, L.; Geng, F.; Wang, D.; Guo, L.-H. *Bioanal. Chem.* **2016**, *408*, 8795.
(22) Yang, D.; He, Y.; Sui, Y.; Chen, F. *Anal. Methods* **2016**, *8*, 7272.
(23) (a) Babudri, F.; Farinola, G. M.; Naso, F. *Synlett* **2009**, 2740. (b) Schlüter, A. D. *J. Polym. Sci. A: Polym. Chem.* **2001**, *39*, 1533.
(24) Maluenda, I.; Navarro, O. *Molecules* **2015**, *20*, 7528.
(25) Akkuratov, A. V.; Susarova, D. K.; Moskvin, Y. L.; Anokhin, D. V.; Chernyak, A. V.; Prudnov, F. A.; Novikov, D. V.; Babenko, S. D.; Troshin, P. A. *J. Mater. Chem. C* **2015**, *3*, 1497.
(26) Liu, S. J.; Zhang, Z. P.; Chen, D. C.; Duan, C. H.; Lu, J. M.; Zhang, J.; Huang, F.; Su, S. J.; Chen, J. W.; Cao, Y. *Sci. China Chem.* **2013**, *56*, 1119.
(27) Wu, J.-S.; Cheng, Y.-J.; Lin, T.-Y.; Chang, C.-Y.; Shih, P.-I.; Hsu, C.-S. *Adv. Funct. Mater.* **2012**, *22*, 1711.
(28) Yoon, J.; Kwag, J.; Shin, T. J.; Park, J.; Lee, Y. M.; Lee, Y.; Park, J.; Heo, J.; Joo, C.; Park, T. J.; Yoo, P. J.; Kim, S.; Park, J. *Adv. Mater.* **2014**, *26*, 4559.
(29) (a) Hohl, B.; Bertschi, L.; Zhang, X.; Schlüter, A. D.; Sakamoto, J. *Macromolecules* **2012**, *45*, 5418. (b) Moscatelli, A.; Livingston, K.; So, W. Y.; Lee, S. J.; Scherf, U.; Wildeman, J.; Peteanu, L. A. *J. Phys. Chem. B* **2010**, *114*, 14430.
(30) Li, J.; Li, M.; Bo, Z. *Chem. Eur. J.* **2005**, *11*, 6930.
(31) **Synthesis of P1**
Tris(dibenzylideneacetone)dipalladium(0) (13.7 mg, 0.015 mmol, 0.15 equiv), potassium carbonate (41.46 mg, 0.3 mmol, 3 equiv), tri(*o*-tolyl)phosphine (9.1 mg, 0.03 mmol, 0.3 equiv), 2,7-dibromofluorenone (compound **5**, 33.8 mg, 0.1 mmol, 1.0 equiv), and 9,9-dioctylfluorene-2,7-diboronic acid bis(1,3-propanediol) ester (compound **4**, 55.8 mg, 0.1 mmol, 1.0 equiv) were added to a round-bottomed flask under an inert nitrogen atmosphere. Toluene (3 mL), 95% ethanol (3 mL), and water (3 mL) were each degassed and added to the flask with a syringe, and the reaction mixture was heated at 50 °C for 72 h under an inert nitrogen atmosphere. The reaction mixture was cooled to r.t. and excess chloroform (approximately 20 mL) was added to the flask. The resulting suspension was filtered by using gravity filtration to remove all palladium byproducts. The organic layer was separated from the aqueous layer, dried over sodium sulfate, filtered, and concentrated with a rotary evaporator. The crude product was precipitated in methanol from chloroform affording a green solid in 96% yield (59.4 mg). M_n = 5000, M_w = 6500, PDI = 1.30. UV absorbance λ_{max} = 374 nm; fluorescence emission λ_{max} = 427 nm, 449 nm; quantum yield = 0.908.
(32) Chen, Z.; Liang, J.; Han, X.; Yin, J.; Yu, G.-A.; Liu, S. H. *Dyes Pigments* **2015**, *112*, 59.
(33) Chang, C.-W.; Soelling, T. I.; Diau, E. W.-G. *Chem. Phys. Lett.* **2017**, *686*, 218.
(34) Ermolaev, N. L.; Lenin, I. V.; Fukin, G. K.; Shavyrin, A. S.; Lopatin, M. A.; Kuznetsova, O. V.; Andreev, B. A.; Kryzhkov, D. I.; Ignatov, S. K.; Chuhmanov, E. P.; Berberova, N. T.; Pashchenko, K. P. *J. Organomet. Chem.* **2015**, *797*, 83.
(35) Cardinal, J. R.; Mukerjee, P. *J. Phys. Chem.* **1985**, *82*, 1614.
(36) Schwarz, F. P.; Wasik, S. P. *Anal. Chem.* **1976**, *48*, 524.
(37) Spano, S. C. *Acc. Chem. Res.* **2010**, *43*, 429.
(38) **Detection Experiment**
A bisphenol solution (0.5 mL, 100, 500, 1000 µM in chloroform or 50, 100 µM in water) was added to a quartz cuvette. A polymer solution (2 mL, 0.01 mg/mL in chloroform or as a nanoparticle solution suspended in water) was added to the cuvette. This sample was then measured with the fluorimeter four times and the average of the four runs was reported. The samples were excited at the polymer's UV-vis absorbance maximum with an excitation slit width of 1.5 nm and emission slit width of 3.0 nm.
(39) Fluorescence modulation = $Fl_{analyte}/Fl_{blank}$
where $Fl_{analyte}$ is the integrated fluorescence emission of the polymer in the presence of the analyte and Fl_{blank} is the integrated fluorescence emission of the polymer in the absence of analyte.
(40) Zhou, Q.; Swager, T. M. *J. Am. Chem. Soc.* **1995**, *117*, 12593.
(41) (a) Huang, L.; Liao, M.; Yang, X.; Gong, H.; Ma, L.; Zhao, Y.; Huang, K. *RSC Adv.* **2016**, *6*, 7239. (b) Guo, H.; Li, H.; Liang, N.; Chen, F.; Liao, S.; Zhang, D.; Wu, M.; Pan, B. *Environ. Sci. Pollut. Res.* **2016**, *23*, 8976.
(42) (a) Szymanski, C.; Wu, C.; Hooper, J.; Salazar, M. A.; Perdomo, A.; Dukes, A.; McNeill, J. *J. Phys. Chem. B* **2005**, *109*, 8543. (b) Potai, R.; Traiphol, R. *J. Colloid Interface Sci.* **2013**, *403*, 58.